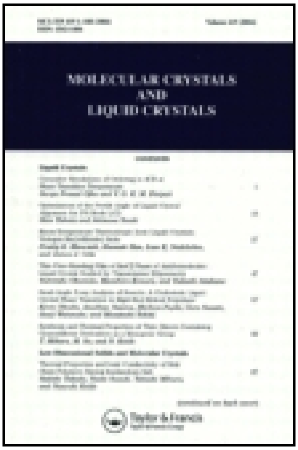

Molecular Crystals and Liquid Crystals

Novel T-shaped Chiral Oligomers with a Wide Temperature Range of a Blue Phase

Masatada Sato [a], Atsushi Yoshizawa [a] & Fumitaka Ogasawara [b]

[a] Department of Frontier Materials Chemistry, Faculty of Science and Technology, Hirosaki University, Hirosaki, Japan

[b] Tohoku Chemical Corporation, Hirosaki, Japan

Version of record first published: 22 Sep 2010

To cite this article: Masatada Sato, Atsushi Yoshizawa & Fumitaka Ogasawara (2007): Novel T-shaped Chiral Oligomers with a Wide Temperature Range of a Blue Phase, Molecular Crystals and Liquid Crystals, 475:1, 99-112

To link to this article: http://dx.doi.org/10.1080/15421400701679939

Mol. Cryst. Liq. Cryst., Vol. 475, pp. 99–112, 2007

ISSN: 1542-1406 print/1563-5287 online
DOI: 10.1080/15421400701679939

Novel T-shaped Chiral Oligomers with a Wide Temperature Range of a Blue Phase

Masatada Sato
Atsushi Yoshizawa
Department of Frontier Materials Chemistry, Faculty of Science and Technology, Hirosaki University, Hirosaki, Japan

Fumitaka Ogasawara
Tohoku Chemical Corporation, Hirosaki, Japan

The crystal structure of (S)-1-methylheptyl-4′-{4-octyloxy-2-{11-[4-(5-hexylpyrimidin-2-yl)phenoxy]undecanoyloxy}benzoyloxy}biphenyl-4-carboxylate, which has a relatively wide temperature range of blue phase III on cooling, has been determined. The molecule was found to form a λ-shaped structure. We have prepared a homologous series of the chiral oligomers and investigated effects of structure on appearance of the blue phase. All compounds were found to show a phase sequence of Iso-BP-N-glass on cooling. The structure-property correlations reveal that (1) chirality does not affect on the Iso-BP transition temperature, (2) increasing chirality destabilizes the N* phase, and (3) the longer spacer lowers the BP-N* transition temperature.*

Keywords: blue phase; chirality; liquid crystal; molecular biaxiality

1. INTRODUCTION

Investigation of chirality in liquid crystals is one of the most exciting areas of liquid crystal science. Frustrated phases induced by chirality are the most interesting phenomena above all. Blue phase (BP), twist grain boundary (TGB) phase and smectic Q (SmQ) phase have been observed and structure-property correlations investigated [1]. Blue

This work was partially supported by Aomori Prefecture Collaboration of Regional Entities for the Advancement of Technological Excellence, JST and a Grant for priority Research Designated by the President of Hirosaki University.

Address correspondence to Atsushi Yoshizawa, Department of Frontier Materials Chemistry, Faculty of Science and Technology, Hirosaki University, 3, Bunkyo-Cho, Hirosaki 036-8561, Japan. E-mail: ayoshiza@cc.hirosaki-u.ac.jp

phases are of particular interest because they have a fluid lattice whose structure is stabilized by lattice defects. Appearance of blue phases results from the competition between the chiral twisting force and the desire for molecules to pack in ways such that they fill space uniformly. Blue phases are believed to consist of double twist cylinder, so are classified into 3 categories depending on packing structure of double twist cylinder, i.e., blue phase I (BPI), blue phase II (BPII) and blue phase III (BPIII). The packing structure of BPI is body−centered cubic structure, and BPII is simple cubic structure. On the other hand, theoretical insights have revealed that BPIII and the isotropic phase have the same symmetry. It can be expected that BPIII consists of double twist cylinders with arbitrary orientation [2]. Usually, blue phases are found in a very narrow temperature range (~ 1K) between the isotropic liquid and the chiral nematic (N^*) phase of sufficiently short pitch, except in a few cases where a SmA to BPI transition has been observed [3–5]. Recently, smectic blue phases (SmBPs) have been observed between the isotropic and smectic phases [6,7]. Yamamoto *et al.* reported novel smectic blue phase 'SmBPIso' in the binary mixture system [8]. Blue phases have the potential of applications as fast light modulators or tunable photonic crystals, but their narrow temperature range is a critical problem. Kikuchi *et al.* reported polymer-stabilized blue phases in which the temperature range is extended to more than 60 K and they demonstrated fast electro-optical switching for the stabilized blue phase [9]. Coles *et al.* reported that eutectic mixtures of three homologues of symmetric dimer doped with a small percentage of a highly twisting chiral additive shows the BPI of a very wide temperature range, and the BPI shows wide color range of reflected color in applied electric fields [10]. On the other hand, many kinds of liquid – crystalline materials possessing a center of chirality have been investigated. A single chiral compound with a wide temperature range of a blue phase has never been obtained. Theoretical work suggests that biaxiality plays an important role in the blue phases [11]. However, the biaxiality in most chiral nematic liquid crystals is slight, thus the double twist structure can not exist in a wide temperature range. We reported a U-shaped molecule that induces a smectic-like layer ordering in the nematic phase and noted possibility that the nematic (N) phase has biaxiality [12]. We designed coupling between axial chirality and the U-shaped system [13–15]. The designed binaphthyl derivatives were found to show an unusual phase sequence of Iso-BP-SmA (Fig. 1(a)). Recently we reported a novel T-shaped chiral oligomer possessing molecular biaxiality exhibiting a blue phase with a wide temperature range on cooling (Fig. 1(b)) [16]. We have prepared a homologous series

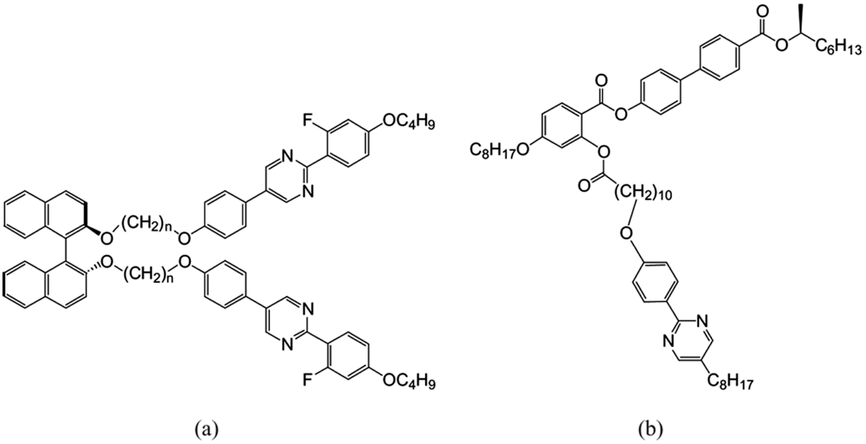

FIGURE 1 Molecular structures of (a) binaphthyl derivatives ***(R)*-n** and (b) T-shaped chiral oligomer **T-1**.

of the T-shaped chiral oligomers and investigated the structure-property relations. In the present study, we report a crystal structure of the T-shaped compound and effects of molecular structure on appearance of a blue phase of the T-shaped compounds.

2. EXPERIMENTAL

Characterization of Materials

The purification of final products was carried out using column chromatography over silica gel (63–210 μm) (KANTO CHEMICAL Co., INC.) using a toluene-ethyl acetate mixture as the eluent, followed by the recrystallization from ethanol. The purity was checked by thin layer chromatography (TLC, aluminum sheets, silica gel 60 F254 from Merck) using a toluene-ethyl acetate mixture as the eluent. Detection of products was achieved by UV irradiation ($\lambda = 254$ and 365 nm).

The structures of the products were elucidated by infrared (IR) spectroscopy (BIO RAD FTS-30) and proton nuclear magnetic resonance (^{1}H-NMR) spectroscopy (JEOL JNM-A400). The analyses of the structures of the products by spectroscopic methods were found to be consistent with the predicted structures.

Preparation of Materials

The T-shaped chiral oligomers (**T-1(m, n), T-2(10, 6)**) were prepared by the synthesis outlined in Scheme 1. (*R*)-2-Octanol was obtained

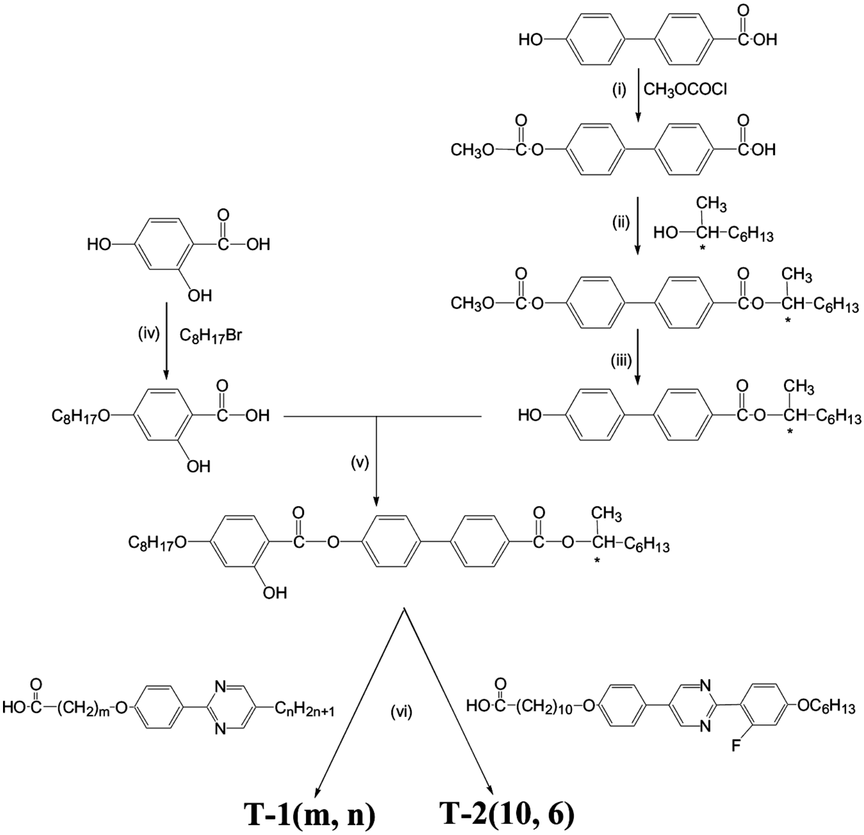

SCHEME 1 The preparative route for the homologous series of the T-shaped chiral oligomers **T-1(m, n) [(m, n) = (9, 8), (5, 8), (10, 6)], T-2(10, 6)**: (i) NaOH, H_2O, then HCl, (ii) DEAD, $(C_6H_5)_3P$, THF, (iii) NH_3(aq), ethanol, (iv) KOH, EtOH-H_2O, and (v) DCC, DMAP, CH_2Cl_2, and (vi) DCC, DMAP, CH_2Cl_2.

from Tokyo Kasei Kogyo Co., Ltd, and (*S*)-2-octanol was obtained from Aldrich. 5-Octyl-2-(4-hydroxyphenyl)pyrimidine was obtained from Midori Kagaku Co., Ltd.

(S)-1-Methylheptyl-4′-{4-octyloxy-2-{10-[4-(5-octylpyrimidin-2-yl)phenoxy]decanoyloxy}benzoyloxy}biphenyl-4-carboxylate, T-1(9, 8)

To a solution of sodium hydroxide (2.8 g, 70 mmol) in water (100 ml), which had been cooled to 0°C, 4-hydroxybiphenyl-4′-carboxylic acid (5.0 g, 23 mmol) was added. The reaction mixture was stirred vigorously and methyl chloroformate (3.9 g, 45 mmol) was added slowly to the resulting suspension. The reaction mixture was stirred at 0°C for 5 h and then brought to pH 2 by the addition of aq. HCl. The voluminous white precipitate produced was filtered off and recrystallized from acetic acid (400 ml). 4-Methoxycarbonyloxybiphenyl-4′-carboxylic acid was obtained. Yield: 5.8 g (92%).

To a solution of 4-methoxycarbonyloxybiphenyl-4′-carboxylic acid (2.5 g, 9.2 mmol) and diethylazodicarboxylate (1.6 g, 9.2 mmol) in tetrahydrofuran (THF, 120 ml) was added triphenylphosphine (2.6 g, 10 mmol) in THF (40 ml). The reaction mixture was stirred at room temperature for 24 h. After the filtration of participate, the solvent was removed by evaporation. The residue was purified by column chromatography on silica gel with dichloromethane. (*S*)-1-methylheptyl-4-methoxycarbonyloxybiphenyl-4′-carboxylate was obtained. Yield: 2.3 g (65%).

To a solution of (*S*)-1-methylheptyl 4-methoxycarbonyloxybiphenyl-4′-carboxylate (2.2 g, 5.8 mmol) in ethanol (95 ml) was added an aqueous ammonia solution (28 ~ 30%, 14 ml). The reaction mixture was stirred at room temperature for 24 h. The solvent was removed by evaporation. To the residue was added water and the solution was extracted with diethylether (100 ml). The combined organic layers were dried over anhydrous sodium sulfate. After the drying agent and the solvent were removed, (*S*)-1-Methylheptyl-4-hydroxybiphenyl-4′-carboxylatewas obtained without further purification. Yield: 1.6 g (85%).

To a solution of 2,4-dihydroxybenzoic acid (7.7 g, 50 mmol) and 1-bromooctane (9.0 g, 47 mmol) in ethanol (70 ml) was added a solution of KOH (10.3 g, 1.85 mol) in water (40 ml). The mixture was stirred under reflux for 10 h. After the solvent was removed, the residue was acidified with aq. HCl. The solution was extracted with diethylether (3 × 50 ml). The organic layers were combined, dried over anhydrous magnesium sulfate, filtered and evaporated. The intermediate product, 2-hydroxy-4-octyloxybenzoic acid, was obtained. Yield: 1.3 g (10%).

To a solution of 2-hydroxy-4-octyloxybenzoic acid (1.0 g, 3.8 mmol) in dichloromethane (30 ml), (*S*)-1-methylheptyl-4-hydroxybiphenyl-4′-carboxylate (1.0 g, 3.1 mmol), dicyclohexylcarbodiimide (0.78 g, 3.8 mmol), and 4-(*N*, *N*-dimethylamino)pyridine (0.047 g, 0.38 mmol) were added. The resulting solution was stirred at room temperature for 30 h. Precipitated materials were removed by filtration. After removal of the solvent by evaporation, the residue was purified by column chromatography on silica gel with toluene as the eluent. (*S*)-1-Methylheptyl-4′-(2-hydroxy-4-octyloxybenzoyloxy)biphenyl-4-carboxylate was obtained. Yield: 1.02 g (47 %).

5-Octyl-2-(4-hydroxyphenyl)pyrimidine (0.57 g, 2.0 mmol) was added in a mixture of ethanol (20 ml) and sodium hydroxide (0.26 g, 6.6 mmol) in water (20 ml). The mixture was heated and stirred while 10-bromodecanoic acid (0.50 g, 2.0 mmol) was added slowly. The reaction mixture was heated under reflux for 7 h. The solvent was removed by evaporation and then the solution was acidified with aq. HCl. The solution was extracted with dichloromethane (3 × 50 ml). The organic layers were combined, dried over anhydrous magnesium sulfate. After the drying agent and the solvent were removed, the desired product was recrystallized from acetic acid (10 ml). 10-[4-(5-Octylpyrimidin-2-yl)phenoxy]decanoic acid was obtained. Yield: 0.23 g (25%).

To a solution of 10-[4-(5-octylpyrimidin-2-yl)phenoxy]decanoic acid (0.18 g, 0.4 mmol) in dichloromethane (10 ml), (*S*)-1-methylheptyl-4′-(2-hydroxy-4-octyloxybenzoyloxy)biphenyl-4-carboxylate (0.18 g, 0.4 mmol), dicyclohexylcarbodiimide (0.083 g, 0.4 mmol), and 4-(*N*,*N*-dimethylamino)pyridine (0.005 g, 0.04 mmol) were added. The resulting solution was stirred at room temperature for 17 h. Precipitated materials were removed by filtration. After removal of the solvent by evaporation, the residue was purified by column chromatography on silica gel with a toluene-ethylacetate (15:1) mixture as the eluent. Recrystallization from ethanol gave the desired product. Yield: 0.17 g (56%).

^{1}H NMR (400 MHz, solvent $CDCl_3$, standard TMS) δ_H/ppm: 8.59(s, 2H, Ar−**H**), 8.36(d, 2H, Ar−**H**, J = 9.3 Hz), 8.21(d, 1H, Ar−**H**, J = 8.8 Hz), 8.13(d, 2H, Ar−**H**, J = 8.3 Hz), 7.67(d, 2H, Ar−**H**, J = 8.8 Hz), 7.66(d, 2H, Ar−**H**, J = 8.3 Hz), 7.27(d, 2H, Ar−**H**, J = 8.6 Hz), 6.99(d, 2H, Ar−**H**, J = 8.8 Hz), 6.89(dd, 1H, Ar−**H**, J = 8.8 Hz, 2.4 Hz), 6.67(d, 1H, Ar−**H**, J = 2.4 Hz), 5.23–5.16(m, 1H, $-C^*\mathbf{H}(CH_3)$), 4.05(t, 2H, $-OC\mathbf{H}_2$, J = 7.1 Hz), 4.02(t, 2H, $-OC\mathbf{H}_2$, J = 6.6 Hz), 2.64-2.60(m, 2H, $Ar-C\mathbf{H}_2-$, 2H, $-OCOC\mathbf{H}_2-$), 1.87–1.31(m, 51H, aliphatic−**H**), 0.93–0.88(m, 9H, $-C\mathbf{H}_3$); IR (KBr) νmax/cm^{-1}: 2927, 2856, 1728, 1613, 1428, 1257, 1135.

The other compounds presented in this paper were obtained by a similar method to that for **T-1(9, 8)**. Analytical data for the other compounds are given.

(S)-1-Methylheptyl-4′-{4-octyloxy-2-{6-[4-(5-octylpyrimidin-2-yl)phenoxy]hexanoyloxy}benzoyloxy}biphenyl-4-carboxylate, T-1(5, 8)

^{1}H NMR (400 MHz, solvent $CDCl_3$, standard TMS) δ_H/ppm: 8.59(s, 2H, Ar−**H**), 8.35(d, 2H, Ar−**H**, J = 9.3 Hz), 8.21(d, 1H, Ar−**H**, J = 8.8 Hz), 8.12(d, 2H, Ar−**H**, J = 8.3 Hz), 7.66(d, 2H, Ar−**H**, J = 8.3 Hz), 7.65(d, 2H, Ar–**H**, J = 8.3 Hz), 7.27(d, 2H, Ar–**H**, J = 8.6 Hz), 6.97(d, 2H, Ar–**H**, J = 8.8 Hz), 6.90(dd, 1H, Ar–**H**, J = 8.0 Hz, 2.7 Hz), 6.68(d, 1H, Ar–**H**, J = 2.4 Hz), 5.24–5.16(m, 1H, $-C^*\mathbf{H}(CH_3)$), 4.05(m, 2H, $-OC\mathbf{H}_2$, J = 5.9 Hz), 4.02(m, 2H, $-OC\mathbf{H}_2$, J = 6.6 Hz), 2.64–2.60(m, 2H, $Ar-C\mathbf{H}_2-$, 2H, $-OCOC\mathbf{H}_2-$), 1.87–1.31(m, 43H, aliphatic–**H**), 0.94–0.89(m, 9H, $-C\mathbf{H}_3$); IR (KBr) ν max/cm^{-1}: 2928, 2857, 1716, 1611, 1430, 1273, 1126.

(S)-1-Methylheptyl-4′-{4-octyloxy-2-{11-[4-(5-hexylpyrimidin-2-yl)phenoxy]undecanoyloxy}benzoyloxy}biphenyl-4-carboxylate, T-1(10, 6)

^{1}H NMR (400 MHz, solvent $CDCl_3$, standard TMS) δ_H/ppm: 8.59(s, 2H, Ar–**H**), 8.36(d, 2H, Ar–**H**, J = 9.3Hz), 8.21(d, 1H, Ar–**H**, J = 9.3Hz), 8.13(d, 2H, Ar–**H**, J = 8.3 Hz), 7.67(d, 2H, Ar–**H**, J = 8.8 Hz), 7.66(d, 2H, Ar–**H**, J = 8.8 Hz), 7.28(d, 2H, Ar–**H**, J = 8.6 Hz), 6.99(d, 2H, Ar–**H**, J = 8.8 Hz), 6.89(dd, 1H, Ar–**H**, J = 8.8 Hz, 2.5 Hz), 6.67(d, 1H, Ar–**H**, J = 2.4 Hz), 5.23–5.16(m, 1H, $-C^*\mathbf{H}(CH_3)$), 4.05(t, 2H, $-OC\mathbf{H}_2$, J = 5.9 Hz), 4.02(t, 2H, $-OC\mathbf{H}_2$, J = 6.4 Hz), 2.62 (t, 2H, $Ar-C\mathbf{H}_2-$, 2H, $-OCOC\mathbf{H}_2-$, J = 7.6 Hz), 1.87–1.31(m, 49H, aliphatic–**H**), 0.94–0.88(m, 9H, $-C\mathbf{H}_3$); IR (KBr) ν max/cm^{-1}: 2926, 2854, 1734, 1613, 1428, 1260, 1131.

(S)-1-Methylheptyl-4′-{4-octyloxy-2-{11-[4-(2-(2-fluoro-4-hexyloxyphenyl)pyrimidin-5-yl)phenoxy]undecanoyloxy}-benzoyloxy}biphenyl-4-carboxylate, T-2(10, 6)

^{1}H NMR (400 MHz, solvent $CDCl_3$, standard TMS) δ_H/ppm: 9.01(s, 2H, Ar–**H**), 8.21(d, 1H, Ar–**H**, J = 8.8 Hz), 8.15–8.10(m, 3H, Ar–**H**), 7.67(d, 2H, Ar–**H**, J = 8.8 Hz), 7.66(d, 2H, Ar–**H**, J = 7.8 Hz), 7.27(d, 2H, Ar–**H**, J = 8.6 Hz), 7.05(d, 2H, Ar–**H**, J = 8.8 Hz), 6.90(dd, 1H, Ar–**H**, J = 8.8 Hz, 2.4 Hz), 6.84(dd, 1H, Ar–**H**, J = 8.8 Hz, 2.4 Hz), 6.76(dd, 1H, Ar–**H**, J = 12.8 Hz, 2.2 Hz), 6.67(d, 1H, Ar–**H**, J = 2.4 Hz), 5.23–5.16(m, 1H, $-C^*\mathbf{H}(CH_3)$), 4.07–4.00(m, 6H, $-OC\mathbf{H}_2$), (t, 2H, $-OCOC\mathbf{H}_2-$, J = 7.6 Hz), 1.87–1.27(m, 47H, aliphatic–**H**), 0.96–0.88(m, 9H, $-C\mathbf{H}_3$); IR (KBr) ν max/cm^{-1}: 2924, 2854, 1737, 1613, 1438, 1246, 1134.

Liquid-Crystalline and Physical Properties

The initial assignments and corresponding transition temperatures for the final products were determined by thermal optical microscopy using a Nikon Optiphoto POL polarizing microscope equipped with a

Mettler FP82 microfurnace and FP80 control unit. The heating and cooling rates were 5°C min^{-1}. Temperatures and enthalpies of transition were investigated by differential scanning calorimetry (DSC) using a Seiko DSC 6200 calorimeter. The material was studied at a scanning rate of 5°C min^{-1}, for both heating and cooling cycles, after being encapsulated in aluminum pans. The helical pitch in the N^* phase was measured by the Cano wedge method for a chiral nematic mixture consisting of nematic liquid-crystalline material, 4-hexyl-4′-cyanobiphenyl (**6CB**) (purchased from BDH) and each chiral additive. The helical pitch in the SmC^* phase was measured by observing a length between the dechirallization lines corresponding to a full pitch band for a mixture consisting of 5-octyloxy-2-(4-hexyloxyphenyl)pyrimidine (**8-PYP-6O**) and each chiral additive. The helical pitches were measured at room temperature. The mixtures were studied using the contact method and their chiral helical twist senses were established. The definition of the helical twist senses used in this article is the same as that of Goodby [17].

Crystal Structure

A single crystal of **T-1(10, 6)** was obtained by slow evaporation methods of an ethanol/n-hexane (1:1) solution. This crystal was mounted on a glass fiber. All measurements were made on a Rigaku RAXIS RAPID imaging plate area detector with graphite monochromated Mo-Kα radiation at room temperature. The structure was solved by applying programs SAPI90 [18] and refined using DIRDIF99 [19].

Crystal data for **T-1(10, 6)**: $\mathrm{C}_{63}\mathrm{H}_{84}\mathrm{O}_8\mathrm{N}_2$, $M = 997.37\,\mathrm{g\,mol}^{-1}$, colorless platelet, $0.50 \times 0.45 \times 0.07\,\mathrm{mm}$, triclinic, space group $P_{\bar{1}}$, $a = 10.699(7)$Å, $b = 15.597(8)$Å, $c = 18.28(1)$Å, $\alpha = 86.42(4)$; $\beta = 84.22(5)$; $\gamma = 81.78(5)$; $V = 3000.4(3)$Å, $Z = 2$, $D_{\mathrm{calc}} = 1.104\,\mathrm{g\ \ cm}^{-3}$, $F000 = 1080.00$, $\mu(\mathrm{MoK}\alpha\ \ ) = 0.72\,\mathrm{cm}^{-1}$, $2\theta_{\max} = 46.5$; 19370 reflections measured, 8549 unique ($R_{\mathrm{int}} = 0.038$), $GoF = 3.64$, $R[I > 3.00\sigma\ (I)] = 0.182$, $R_{\mathrm{w}}[I > 3.00\sigma\ (I)] = 0.173$.

3. RESULTS AND DISCUSSION

3.1. Crystal Structure

Figure 2 shows molecular structure of **T-1(10, 6)** exhibiting blue phase and N^* phase (see Table 1). The final R-value is relatively high (0.182) due to disorder. The terminal alkyl chains were not determined. The compound was found to have a λ-shaped structure instead of T-shaped.

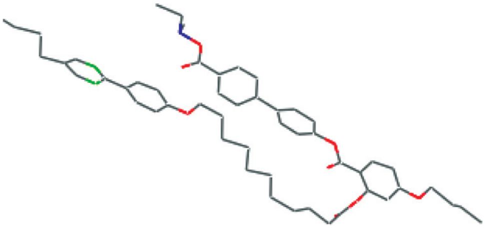

FIGURE 2 Molecular structure of **T-1(10, 6)** viewed along the *a* axis.

Gauche configurations exist in the central spacer. Owing to MM2 calculations, the λ-shaped structure is more stable than the T-shaped and the energy difference between them is estimated to be $31\,\mathrm{kJ\,mol^{-1}}$. Figure 3 shows crystal structure of **T-1(10, 6)**. The molecules are almost antiparallel to each other, giving a smectic-like layer structure in which the molecules are tilted to the layer normal.

3.2. Liquid-Crystalline Properties and Pitch Measurements

Molecular structures of T-shaped chiral oligomer **T-1(m, n)** and **T-2(10, 6)** are shown in Figure 4. Temperatures and enthalpies of the transition for the homologous series of T-shaped chiral oligomers **T-1(m, n)** and **T-2(10, 6)** determined by optical microscopy and differential scanning calorimetry (DSC) are listed in Table 1.

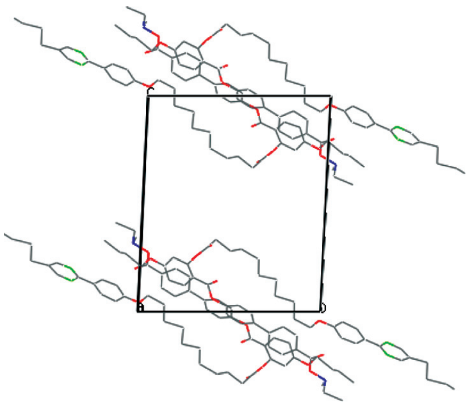

FIGURE 3 Crystal structure of **T-1(10, 6)** viewed along the *a* axis.

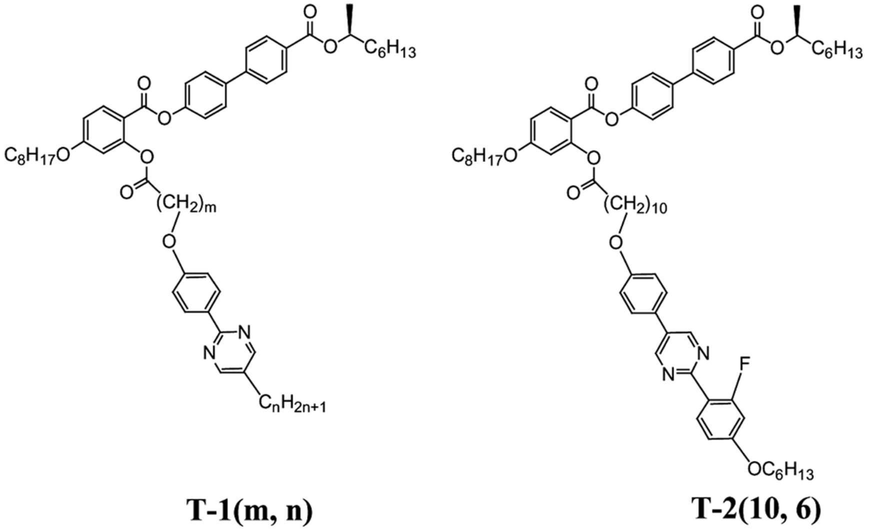

FIGURE 4 Molecular structures of T-shaped chiral oligomers **T-1(m, n)** and **T-2(10, 6)**.

All T-shaped chiral oligomers were found to show a phase sequence of Iso-BP-N*-glass on cooling. All the liquid crystal phases of these mesogens are monotropic. The texture of the blue phase is blue fog texture without any platelet texture, indicating that the blue phase is BPIII. The spacer length (m) and terminal chain length (n) slightly affected on stability of the blue phase. As the spacer length (m) was shorter, the temperature range of the blue phase was narrower. Interesting odd-even effect was observed for appearance of a blue phase of some chiral dimeric liquid crystals [20]. However, the present chiral

TABLE 1 Transition Temperatures (°C) on Cooling and Enthalpies ($kJ\,mol^{-1}$) of Transition (in Brackets) for **T-1(m, n)** and **T-2(10, 6)**

	glass[a]	N*[b]	BP	I	mp[a]
T-1(10, 8)	• – 25	•15	•28 (1.4)	•	63 (66)
T-1(9, 8)	• – 23	•19	•28 (1.2)	•	45 (48)
T-1(5, 8)	• – 19	•28	•32 (0.6)	•	68 (53)
T-1(10, 6)	• – 22	•14	•25 (1.4)	•	40 (47)
T-2(10, 6)	• – 16	•72	•77 (0.7)	•	80 (45)

[a] The melting points and glass transition temperatures were measured by DSC.
[b] Enthalpies of the BP to N* transition were too small to be detected.

TABLE 2 Helical Pitch (μm) in the N* and SmC* Phases for a Mixture Consisting of 2 wt% of each Chiral Compound and the Helical Twist Senses (in Brackets), i.e., Right-hand (RH) or Left-hand (LH)[a]

Compound	SmC*	N*
T-1(10, 8)	20 (RH)	7.0 (RH)
T-1(9, 8)	18 (RH)	8.5 (RH)
T-1(5, 8)	54 (RH)	7.0 (RH)
T-1(10, 6)	22 (RH)	7.0 (RH)
T-2(10, 6)	23 (RH)	10 (RH)

[a] Helical pitch (μm) in the N* phase for a chiral nematic mixture of **6CB** and 2 wt% of each chiral compound and that in the SmC* phase for a chiral mixture of **8-PYP-6O** and 2 wt% of each chiral compound were observed at room temperature.

oligomers did not show the odd-even effect. From the crystal study, gauche and trans configurations coexist in the central spacer of **T-1(10, 6)**. Thus parity of the spacer does not play an important role in the molecular structure. **T-2(10, 6)** possessing a [2-(2-fluoro-4-hexyloxyphenyl)pyrimidine-5-yl]phenyl unit was found to show the markedly higher Iso-BP transition temperature than **T-1(10, 6)**. The higher Iso-BP transition temperature can be attributed to the increase of liquid crystallinity of **T-2(10, 6)** having the three ring unit.

Table 2 shows the helical pitch values and helical twist sense in the N* and SmC* phases of each chiral compound.

Pitch measurements reveal that there is no significant difference in the twisting power in the N* phase among the present compounds. The crystal structure suggests that the **T-1(10, 6)** exists as a λ-shaped structure rather than a T-shaped structure. Thus **T-1(10, 6)** is thought to have two possible molecular long axes, *i.e.* an axis through the biphenylbenzoate unit and the other through the phenylpyrimidine unit. We can say that **T-1** has molecular biaxiality. **T-1(5, 8)** with the shorter central spacer showed the higher BP-N* transition. Flexibility of **T-1(5, 8)** is thought to be less than that of **T-1(10, 6)**. Decreasing the flexibility can decrease the molecular biaxiality.

3.3. Miscibility Studies

We investigated chiral effect on the transition behavior of **T-1(10, 8)**. Figure 5 shows a binary phase diagram on cooling of (***S***)**T-1(10, 8)** and its isomer (***R***)**T-1(10, 8)**. The transition temperatures were determined by optical microscopy.

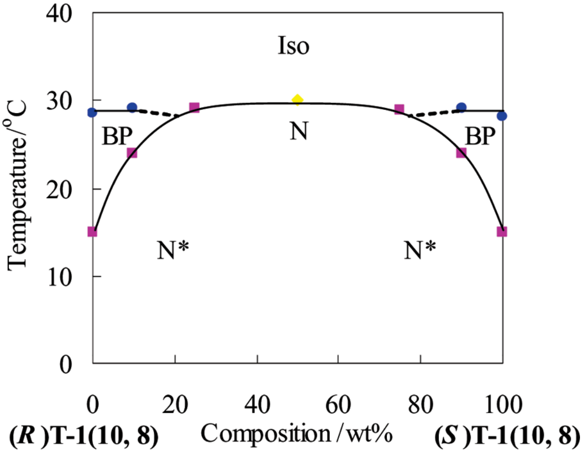

FIGURE 5 Binary phase diagram on cooling for mixtures of (***R***)**T-1(10, 8)** and (***S***)**T-1(10, 8)**.

On decreasing the optical purity, the Iso-BP transition temperature did not change, however, the BP-N* transition temperature increased markedly. The blue phase was found to disappear as the percentage of the isomer rose above 25 wt%.

In order to stabilize the blue phase, we investigated transition behavior of binary mixtures between **T-1(10, 8)** and **T-2(10, 6)**. The phase diagram on cooling is shown in Figure 6(a). The blue phase of both materials proved to be miscible across the full composition range,

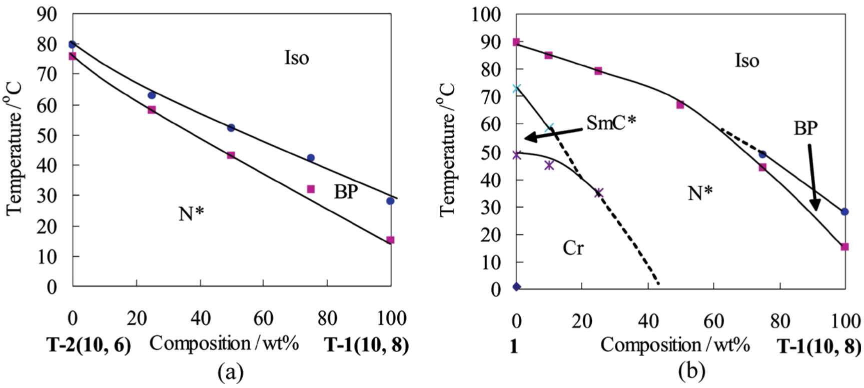

FIGURE 6 (a) Binary phase diagram on cooling for mixtures of **T-1(10, 8)** and **T-1(10, 6)**, and (b) binary phase diagram on cooling for mixtures of **T-1(10, 8)** and **1**.

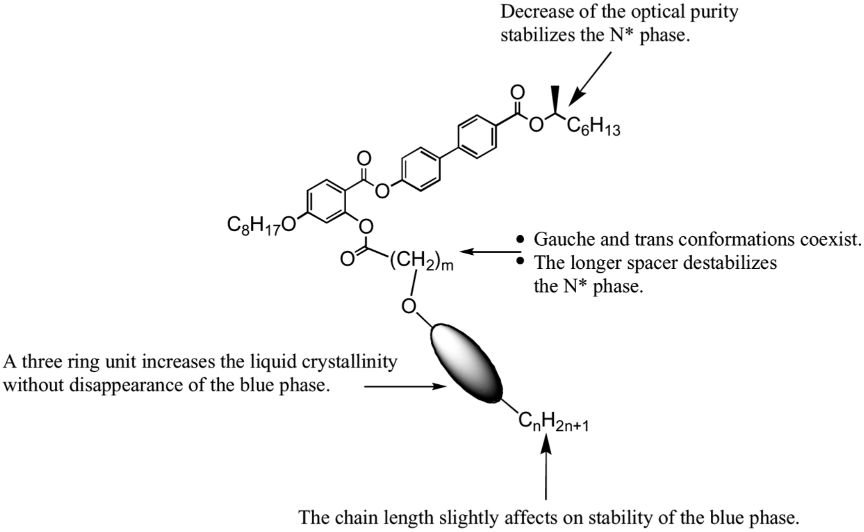

Decrease of the optical purity stabilizes the N* phase.

- Gauche and trans conformations coexist.
- The longer spacer destabilizes the N* phase.

A three ring unit increases the liquid crystallinity without disappearance of the blue phase.

The chain length slightly affects on stability of the blue phase.

FIGURE 7 Structure-property correlations for the T-shaped chiral liquid-crystalline oligomers on appearance of the blue phase.

however, the temperature range of the blue phase was not extended. Figure 6(b) shows a phase diagram between **T-1(10, 8)** and achiral compound **1**.

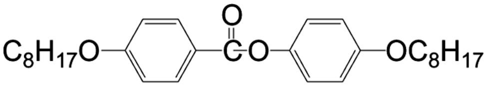

1

Iso 89.4 N 73 SmC 49 Cr

The blue phase was observed for a mixture containing 75 wt% of **T-1(10, 8)**. The Iso-BP transition temperature of the mixture is higher than that of **T-1(10, 8)**, however, the marked increase of the BP-N* transition temperature of the mixture decreases a temperature range of the blue phase. The change of the BP-N* transition temperature across the diagram is explainable by two reasons, i.e. (1) BP-N* transition temperature of **T-1(10, 8)** is not the same as Iso-N transition temperature of compound **1**, and (2) the chirality is changing across the diagram.

The miscibility studies reveal that (1) a high degree of chirality destabilizes the N* phase and (2) the blue phase can be stabilized by doping achiral nematic material which has higher Iso-N transition temperature than T-shaped chiral oligomer.

4. CONCLUSIONS

We have prepared the homologous series of the T-shaped chiral liquid crystalline oligomers and investigated effects of molecular structure on appearance of the blue phase. The crystal structure study suggest that (1) the oligomer forms a λ-shaped structure, (2) gauche and trans configurations coexist in the central spacer, and (3) the molecules are almost antiparallel to each other. The structure-property correlations are summarized in Figure 7. Coupling of chirality and molecular biaxiality of the λ-shaped chiral oligomer can induce the double twist structure of the blue phase by destabilizing the uniaxial helix of the N^* phase.

REFERENCES

[1] Goodby, J. W. (1998). *Handbook of Liquid Crystals Vol 1*, Demus, D., Goodby, J. W., Gray, G. W., Spiess, H. -W., & Vill, V. (Eds.), Chapter V, Wiley-VCH: Weinheim, 115.

[2] Crooker, P. P. (2001). *Chirality in Liquid Crystals*, Kitzerow, H. S. & Bahr, C. (Eds.), Chapter 7, Springer: New York, 212–218.

[3] Onusseit, H. & Stegemeier, J. (1984). *Z. Naturforsch. Teil A.*, *392*, 658.

[4] Nguyen, H. -T., Sallen, C., Babeau, A., Galvan, J. M., & Destrade, C. (1987). *Mol. Cryst. Liq. Cryst.*, *154*, 147.

[5] Vashchenko, V. V., Kutulya, L. A., Pivenko, M. N., & Shkolnikova, N. I. (2003). *Russian hem. Bull. Int. Ed.*, *52*, 2406.

[6] Pansu, B., Grelet, E., Li, M. H., & Nguyen, H. T. (2000). *Phys. Rev. E.*, *62*, 658.

[7] Takanishi, Y., Ogasawara, T., Yoshizawa, A., Umezawa, J., Kusumoto, T., Hiyama, T., Ishikawa, K., & Takezoe, H. (2002). *J. Mater. Chem.*, *12*, 1325.

[8] Yamamoto, J., Nishiyama, I., Inoue, M., & Yokoyama, H. (2005). *Nature*, *437*, 525.

[9] Kikuchi, H., Yokota, M., Hisakado, Y., Yang, H., & Kajiyama, T. (2002). *Nature Materials*, *1*, 64.

[10] Coles, H. J. & Pivnenko, M. N. (2005). *Nature*, *436*, 997.

[11] Wright, D. C. & Mermin, N. D. (1989). *Modern Physics*, *61*, 385.

[12] Yoshizawa, A. & Yamaguchi, A. (2002). *Chem. Commun.*, 2060.

[13] Rokunohe, J. & Yoshizawa, A. (2005). *J. Mater. Chem.*, *15*, 275.

[14] Rokuhone, J., Yamaguchi, A., & Yoshizawa, A. (2005). *Liq. Cryst.*, *32*, 207.

[15] Yoshizawa, A., Rokunohe, J., Segawa, S., & Ogasawara, F. (2006). *Proc. of SPIE.*, *6135*, 613508.

[16] Yoshizawa, A., Sato, M., & Rokunohe, J. (2005). *J. Mater. Chem.*, *15*, 3285.

[17] Goodby, J. W. (1991). *J. Mater. Chem. 1*, 307.

[18] Hai-Fu, F. (1990). SAPI90 program for crystal structure determination, Rigaku Corporation: Tokyo, Japan.

[19] Beurskens, P. T., Admiraal, G., Beurskens, G., Bosman, W. P., de Gelder, R., Israel, R., & Smits, J. M. M. (1999). DIRDIF-99 program system, University of Nijmegen: Netherlands.

[20] Blatch, A. E., Fletcher, I. D., & Luckhurst, G. R. (1997). *J. Mater. Chem.*, *7*, 9.